

Numerical Modeling of the Formation of Aerosol Particles in Jet Engine Plumes

A. B. Vatazhin, V. E. Kozlov, A. M. Starik, and E. K. Kholshchevnikova

Received May 30, 2006

Abstract—The formation of liquid sulfate aerosols in the isobaric axisymmetric plume of a subsonic aircraft is modeled numerically. The specific features of the appearance and evolution of sulfate aerosols attributable to 2D effects, such as the parameter nonuniformity in the initial section (at the nozzle outlet), mixing of the hot engine jet with the cold air stream, and the transverse turbulent diffusion of aerosol particles and gas mixture components. The equations of gas dynamics for a turbulent axisymmetric jet, the equations of chemical kinetics, the equations for the liquid fractions (water and sulfuric acid), and the relations for the binary nucleation, condensation growth and coagulation of aerosol particles are used. The distributions of the parameters determining the formation of the aerosol phase in the exhaust plume of a B-747 aircraft are obtained and the geometry of the nucleation zone in this plume is determined.

DOI: 10.1134/S0015462807010048

Keywords: axisymmetric plume, aircraft engines, chemical kinetics, binary nucleation, sulfate aerosols.

The aerosols formed in jet engine plumes can significantly affect the atmospheric aerosol composition, the radiation balance, and the climate [1–3]. Measurements show that most of the aerosol particles emitted by aviation into the atmosphere (80–90%) are liquid sulfate aerosols with a particle size on the range 1–10 nm [4–8]. In recent years, on the basis of intense numerical and experimental studies considerable progress has been made in understanding the mechanisms of formation of these aerosols in the wakes of sub- and supersonic aircraft [7–17]. Detailed physico-chemical models of aerosol particle formation have been developed, making it possible to determine the evolution of the particle size distribution function and the particle composition [9–17]. Thus, it has been demonstrated that the presence of a considerable concentration of fairly coarse sulfate aerosols with a diameter $d > 5$ nm in the plume ($\sim 10^8 \text{ cm}^{-3}$) can be partially explained by the conversion of sulfur dioxide SO_2 , the main S-containing component of the combustion products of aviation kerosene, into SO_3 and H_2SO_4 in the engine duct and over a significant portion of the engine plume [8, 16, 17], and also by the effect of the ions formed in the high-temperature zone of the combustion chamber on the coagulation of the fine aerosol particles with $d = 1\text{--}2$ nm formed in the plume as a result of nucleation and condensation.

In some cases, good agreement between the calculations and the experimental data was obtained. However, some questions still remain. Thus, for example, for the cruising flight regime of a typical subsonic passenger aircraft almost all the modern models predict the appearance of aerosol particles at distances greater than 40 m from the engine nozzle exit. At the same time, experiments show that liquid aerosols may be formed much earlier, at distances of about 20–30 m from the nozzle exit [6]. The influence of ions and organic combinations emitted from the combustion chamber on the formation of aerosol particles and the role of sulfate aerosols in the formation of ice particles and the visible aircraft wake are still unclear.

Although, for describing the specific features of aerosol formation detailed physico-chemical models were used, the hydrodynamic processes were considered within the framework of simplified zero-dimensional [8–13] or quasi-one-dimensional [14–17] models. Some attempts have been made to take into account the nonuniform distribution of the chemical composition of the mixture and the aerosol concentration in the turbulent plume on the basis of calculations of the physico-chemical processes along the

stream tubes, whose location, together with the variation of the density, temperature, and velocity, had been found earlier from the solution of the hydrodynamic problem. Clearly, in this approach the diffusion effects and their influence on the formation of the condensed phase are not taken into account. However, as early as in [18] it was noted that the hydrodynamic nonuniformities can significantly affect the aerosol distribution in isobaric turbulent vapor-air jets. Calculations [19] showed that the chemical processes in these jets are in great measure determined by the transverse gradients of the concentrations of the reacting components.

The aim of this paper is to analyze the effects of flow nonuniformities in subsonic-aircraft jet engine plumes on the dynamics of sulfate aerosol formation in the plumes. These effects are attributable to the nonuniform distribution of the parameters at the engine nozzle outlet, the mixing of the gas flowing out of the nozzle with the cold atmospheric air, and the transverse diffusion of the mixture components and the aerosol particles in the plume.

1. PHYSICO-MATHEMATICAL MODEL

For calculating the dynamics of formation of sulfate aerosols in the axisymmetric exhaust plume of a jet engine, we will use the assumption that the chemical and condensation processes do not affect the gasdynamic parameters of the flow (the velocity, density, and gas temperature distributions) [20]. This is because, at the nozzle outlet, the molar fractions of all the components of the gas mixture, except for N_2 and O_2 , are fairly or very small (the molar fraction of the water vapor participating in the formation of the aerosol amounts to 0.04 and the molar concentration of the sulfuric acid vapor, which also participates in this process, is even smaller). Preliminary calculations of the processes in the jet engine exhaust plume performed with and without taking the effect of chemical and condensation processes on the gasdynamic parameters into account gave almost the same result. This makes it possible to consider the chemical reactions and the formation of the condensed phase against the background of independently calculated distributions of the gasdynamic parameters. Thus, the general system of equations contains the gasdynamic equations of chemical kinetics for the mixture components and the equations for the dispersed phase with account for particle coagulation.

Gasdynamic Equations

For a turbulent axisymmetric isobaric jet, the equations of conservation of mass, momentum, and energy, and the turbulent viscosity equation take the form (see, for example, [21]):

$$\begin{aligned} \frac{\partial(\rho u)}{\partial x} + \frac{\partial(\rho v)}{\partial r} &= 0, \quad \rho u \frac{\partial u}{\partial x} + \rho v \frac{\partial u}{\partial r} = \frac{1}{r} \frac{\partial}{\partial r} \left(\rho r \varepsilon \frac{\partial u}{\partial r} \right), \\ \rho u \frac{dh_0}{\partial x} + \rho v \frac{\partial h_0}{\partial r} &= \frac{1}{r} \frac{\partial}{\partial r} \left(\frac{\rho r \varepsilon}{\text{Pr}} \frac{\partial h_0}{\partial r} \right) + \left(1 - \frac{1}{\text{Pr}} \right) \frac{1}{r} \frac{\partial}{\partial r} \left[\rho r \varepsilon \frac{\partial}{\partial r} \left(\frac{u^2}{2} \right) \right], \\ h_0 &= h + \frac{u^2}{2}, \quad h = \frac{k}{k-1} \frac{p}{\rho}, \\ \rho u \frac{\partial \varepsilon}{\partial x} + \rho v \frac{\partial \varepsilon}{\partial r} &= \frac{1}{r} \frac{\partial}{\partial r} \left(2 \rho r \varepsilon \frac{\partial \varepsilon}{\partial r} \right) + \alpha^* \rho \varepsilon \left| \frac{du}{dr} \right|, \quad \alpha = 0.2 - \frac{5\varepsilon}{a^2} \left| \frac{\partial u}{\partial r} \right|. \end{aligned} \quad (1.1)$$

Here, x and r are the coordinates in the axisymmetric jet, u and v are the corresponding velocity components, p and ρ are the gas pressure and density, ε is the turbulent viscosity, a is the sonic velocity, and h is the enthalpy of the mixture. In the general case, the quantity h should include the contributions of all the components of the gas mixture and the condensed phase. However, since the concentration of the aerosol particles in the plume ($\sim 10^{10} \text{ cm}^{-3}$) is small as compared with the concentration of the molecular components ($\sim 10^{19} \text{ cm}^{-3}$) and the mass of the condensed phase is also small, the contribution of the condensed phase to the enthalpy of the mixture may be neglected. Since only components with molar fractions less than

10^{-4} are formed in the plume and the heat release due to chemical reactions is negligibly small, the perfect gas approximation holds. For a mixture of hydrocarbon fuel combustion products and air (this mixture is typical of the jet engine exhaust plume), we may with good accuracy assume that $k = 1.4$.

The turbulent Prandtl number Pr was taken equal to 0.7. The last of Eqs. (1.1) describes the variation of the turbulent viscosity ε in accordance with the one-parameter turbulence model [21]. System (2.1) is integrated for given boundary conditions for the gasdynamic parameters and the turbulent viscosity at the nozzle outlet and in the ambient atmosphere.

Equations of Chemical Kinetics

We will consider the process of formation of sulfate aerosols which appear in the gas phase as a result of binary volume nucleation of the H_2O and H_2SO_4 vapor and the subsequent condensation of these components of the gas mixture on the nuclei formed. Since the nucleation and condensation result in a change in the concentration of H_2O and H_2SO_4 in the gas phase and hence in a change in the rates of the reactions in which these components participate, the equations of chemical kinetics should be integrated together with the equations describing the onset and evolution of the condensed phase. The formation of sulfate aerosols may also affect the concentrations of the other chemical components [20].

The system of equations of chemical kinetics describing the variation of the number concentration N_i of the i -th component of the mixture due to chemical reactions and the transition of the component in question into the condensed phase takes the form:

$$\begin{aligned} \rho u \frac{\partial(N_i/\rho)}{\partial x} + \rho v \frac{\partial(N_i/\rho)}{\partial r} &= \frac{1}{r} \frac{\partial}{\partial r} \left[\frac{\rho r \varepsilon}{Sc} \frac{\partial(N_i/\rho)}{\partial r} \right] + (G_i - J_{ci}), \\ G_i &= \sum_{q=1}^L S_{iq}, \quad S_{iq} = (\alpha_{iq}^- - \alpha_{iq}^+)(R_q^+ - R_q^-), \\ R_q^{+(-)} &= k_q^{+(-)} \prod_{j=1}^{n_q^{+(-)}} N_j^{\alpha_{jq}^{+(-)}}. \end{aligned} \quad (1.2)$$

Here, L is the number of chemical reactions resulting in the formation (decomposition) of the i -th component, $\alpha_{iq}^{+(-)}$ are the stoichiometric coefficients of the forward (+) and back (−) q -th chemical reaction, J_{ci} characterizes the total rate of transition of the i -th component into the condensed phase as a result of spontaneous (homogeneous) nucleation and heterogeneous condensation ($i = 1$ and 2 for H_2O and H_2SO_4 , $J_{ci} = 0$ for $i > 2$), and Sc is the turbulent Schmidt number, which for subsonic isobaric jets is assumed to be equal to 0.7.

The kinetic model of the nonequilibrium chemical processes in the engine plume included 59 reactions with account for 20 ($1 \leq i \leq 20$) components: O , O_2 , O_3 , H , H_2 , OH , HO_2 , H_2O , N_2 , NO , NO_2 , NO_3 , N_2O_5 , HNO , HNO_2 , HNO_3 , SO_2 , SO_3 , HSO_3 , and H_2SO_4 . This model was obtained by reducing a more complete scheme developed in [22] for analyzing photochemical processes in jet engine plumes, which makes it possible to consider the chemical transformations in the plume attributable not only to the cooling of the combustion products but also to the mixing of these components with air containing small atmospheric components, including those which influence the formation of H_2SO_4 in the plume.

Equations for the Dispersed Phase

In addition to nucleation and condensation growth, drop formation in the jet engine plume depends significantly on the coagulation of the drops [10–17].

Coagulation changes the spectrum (sizes) of the drops and the drop concentration and may indirectly influence the condensation fluxes of H_2O and H_2SO_4 molecules and, as a result, even the mass of the liquid

phase. We note that in earlier studies devoted to the analysis of condensation in axisymmetric isobaric vapor-air jets [18, 23], coagulation was not taken into account.

In this study, for taking the coagulation growth of the aerosol particles into account, we will use a simplified approach developed in [24] which makes it possible to separate the equations for the mass fractions of H_2O and H_2SO_4 in the liquid phase and for the concentration of liquid drops. In so doing, we assume that at each point of space only particles of the same size (monodisperse group) are present. This approximation makes it possible to gain information about a certain mean particle size which varies with the gas parameters and the concentrations of H_2O and H_2SO_4 in the mixture. In this case, the equations for the variation of the mass concentrations α_{1L} and α_{2L} of the liquid phases of H_2O and H_2SO_4 can be written as follows:

$$\begin{aligned}\rho u \frac{\partial \alpha_{1L}}{\partial x} + \rho v \frac{\partial \alpha_{1L}}{\partial r} &= \frac{1}{r} \frac{\partial}{\partial r} \left(\frac{\rho r \varepsilon}{\text{Sc}} \frac{\partial \alpha_{1L}}{\partial r} \right) + m_* I_n (1 - z_*) + \rho \Omega J_1, \\ \rho u \frac{\partial \alpha_{2L}}{\partial x} + \rho v \frac{\partial \alpha_{2L}}{\partial r} &= \frac{1}{r} \frac{\partial}{\partial r} \left(\frac{\rho r \varepsilon}{\text{Sc}} \frac{\partial \alpha_{2L}}{\partial r} \right) + m_* I_n z_* + \rho \Omega J_2.\end{aligned}\quad (1.3)$$

Here, m_* is the critical-nucleus mass, I_n is the nucleation rate, z_* is the mass fraction of sulfuric acid in the critical nucleus, J_1 and J_2 are the vapor condensation rates for H_2O and H_2SO_4 , respectively, and $\Omega = N_d/\rho$, where N_d is the drop number concentration per unit volume. The variation of the quantity Ω is described by the following equation:

$$\rho u \frac{\partial \Omega}{\partial x} + \rho v \frac{\partial \Omega}{\partial r} = \frac{1}{r} \frac{\partial}{\partial r} \left(\frac{\rho r \varepsilon}{\text{Sc}} \frac{\partial \Omega}{\partial r} \right) + I_n - K_C \rho^2 \Omega^2. \quad (1.4)$$

The coagulation constant was calculated using the formula [15]

$$\begin{aligned}K_C &= 4\pi(r_{d1} + r_{d2})(D_1 + D_2)f(\text{Kn}), \\ f(\text{Kn}) &= \frac{1 + \text{Kn}}{\gamma + 2\text{Kn}(1 + \text{Kn})}, \quad \text{Kn} = 2\sqrt{\frac{\pi\mu}{8RT}} \frac{D_1 + D_2}{r_{d1} + r_{d2}}.\end{aligned}$$

Here, r_{d1} and r_{d2} are the radii of the colliding aerosol particles, D_1 and D_2 are their diffusion coefficients, $f(\text{Kn})$ is the Knudsen correction which takes into account the rarefaction of the medium as the drop size decreases, R is the universal gas constant, and γ is the particle adhesion coefficient in the collision (as in [15], we assumed that $\gamma = 1$).

The nucleus parameters m_* and z_* and the $\text{H}_2\text{O}/\text{H}_2\text{SO}_4$ binary nucleation rate I_n were calculated with account for hydrate formation on the basis of the classical nucleation theory using the formulas given in [20]. The vapor condensation rates J_1 and J_2 for H_2O and H_2SO_4 were determined from the Hertz–Knudsen formula

$$J_i = \frac{\alpha_{vi} 4\pi r_d^2 [p_i - p_{is}(T, z, r_d)]}{\sqrt{2\pi RT/\mu_i}} \quad (i = 1, 2), \quad (1.5)$$

$$p_{is}(T, z, r_d) = p_{is}^\infty(T, z) \exp\left(\frac{2\sigma(z)\mu_i}{r_d(z)\rho_i RT}\right). \quad (1.6)$$

Here, r_d is the drop radius (its value is found using the drop mass and the density of the $\text{H}_2\text{O}/\text{H}_2\text{SO}_4$ solution in the drop), z is the mass fraction of H_2SO_4 in the drop, p_i is the partial pressure of the i -th component over a plane surface of the solution with a mass fraction of H_2SO_4 equal to z at the temperature T , ρ_i and μ_i are the density and the molecular mass of the i -th component, and α_{vi} is the condensation coefficient of the vapor of the i -th component on the sulfate particle surface. In accordance with the recommendations of [14], we assumed that $\alpha_{v1} = 1$ and $\alpha_{v2} = 0.09$. All the molecular constants and coefficients necessary for the calculations and the dependences p_{is}^∞ and $\sigma(z)$ were taken to be the same as in [20].

The solution of system (1.1)–(1.6) was found numerically using an explicit-implicit finite-difference scheme of the first order in the longitudinal coordinate and the second order in the transverse coordinate. The method of solving these equations was described in [25].

The main characteristic of the model considered is the fact that it takes into account the effects of lateral turbulent diffusion of the chemical components and the drops on the dynamics of condensed phase formation. However, in contrast to the quasi-one-dimensional models [14–17] proposed earlier, the condensation model considered here does not make it possible to determine the size distribution of the drops.

2. THE RESULTS OF NUMERICAL MODELING

The dynamics of sulfate aerosol formation were analyzed for the specific case of a B-747 jet engine plume in the cruising flight regime (height $H = 10.7$ km and Mach number $M_0 = 0.8$). The boundary conditions for the calculations were the gas parameters (temperature, pressure, velocity, and gas composition) at the nozzle outlet and in the ambient space. The B-747 is fitted with two-duct turbojet engines, for example CF6-80, for which the diameter of the main (first) duct is $d_I = 87.6$ cm and that of the outer (second) duct $d_{II} = 175.1$ cm. The gasdynamical parameters at the nozzle outlet for the first and the second ducts are, respectively: $T_I = 598$ K, $u_I = 475.7$ m/s and $T_{II} = 253.4$ K and $u_{II} = 316.3$ m/s. At the nozzle outlet the pressure is equal to atmospheric: $p_I = p_{II} = p_0 = 23930$ Pa. The temperature and velocity in the wake are $T_0 = 219.2$ K and $u_0 = 237$ m/s. The composition of the mixture at the main duct nozzle outlet was taken from [17]. We note that this composition was calculated by integrating the one-dimensional gasdynamic equations in the engine duct with account for nonequilibrium chemical reactions in the combustion chamber, the turbine, and the nozzle. For the second duct, the air composition corresponding to atmospheric conditions at a height $H = 10.7$ km was also taken from [17]. The table shows the values of the flow parameters and the concentrations of the different components in molar fractions at the nozzle outlet for two values of the mass percentage of sulfur in the fuel $[S]_f = 0$ and 0.04% and in the atmosphere. It was assumed that the concentration of sulfate aerosols in the atmosphere at the height considered is negligibly small: $N_{d\infty} = 0$. The turbulent viscosity was taken equal to $2.5 \times 10^{-4} u_I d_I$ at the nozzle outlet and $2.5 \times 10^{-10} u_I d_I$ in the outer flow. (The value of ε was chosen from the following considerations. It is known that $\varepsilon \sim 0.1 L u'$, where L is the turbulence scale and u' is the velocity fluctuation intensity. It is commonly assumed that at the jet engine nozzle outlet $L/d_I \sim 0.1$ and $u'/u_I \sim 0.025$. Accordingly, at the outlet we obtain the first of the above values of ε . In the external stream, the turbulent viscosity should be smaller than the molecular viscosity. The second of the above values of ε satisfies this condition.) From the table, it is clear that, for both $[S]_f = 0\%$ and $[S]_f = 0.04\%$, the main S-containing component at the nozzle outlet of the main engine duct is SO_2 . At the nozzle outlet, there is also a noticeable concentration of sulfuric acid vapor. It is important to note that even if the fuel contains no sulfur, the concentration of these components in the engine exhaust is much greater than that in the atmosphere. This is attributable to the oxidation of CS_2 , COS , H_2S , and SO_2 in the engine combustion chamber which these components enter together with atmospheric air [17].

The presence of H_2SO_4 at the nozzle outlet even when $[S]_f = 0\%$ indicates that, even for fuels which do not contain sulfur or its compounds, for example, for hydrogen or methane, sulfate aerosols may be formed in the exhaust plume. The necessary condition for the formation of these particles (in the first stage, nuclei or nucleation centers) is the presence of regions in which the saturation coefficients are greater than unity. For binary nucleation, two saturation coefficients S_1 and S_2 are introduced. They are defined as the ratios of the partial pressures of the water vapor and sulfuric acid vapor to their equilibrium values over a plane surface of the $\text{H}_2\text{O}/\text{H}_2\text{SO}_4$ solution. Figure 1 shows the variation of S_1 (supersaturation in H_2O) with the radius in different sections of the plume. Clearly, in the H_2O vapor supersaturation (S_1) is attained only at the periphery of the plume in a fairly narrow layer $3 < r < 5$ (here and in what follows, the nondimensional values of the radius $r' = 2r/d_I$ are given and, where possible, the prime is omitted) and at fairly large distances from the nozzle outlet ($x = 40\text{--}60$ m). The maximum value of S_1 is not greater

Table

Parameter/Component	Duct I		Duct II/Atmosphere
T , [K]	598		253.4/219.2
p , [Pa]	23 930		23 930
r , [m]	0.438		0.875
u , [m/s]	475.7		316.3/237
Composition	$[S]_f = 0\%$	$[S]_f = 0.04\%$	
O	2.85(−8)	6.58(−8)	1.664(−15)
O ₂	1.54(−1)	1.54(−1)	2.002(−1)
O ₃	2.30(−8)	5.65(−8)	7.275(−8)
H	1.23(−14)	4.63(−14)	2.35(−20)
H ₂	3.09(−8)	2.15(−8)	9.378(−7)
OH	2.01(−6)	2.22(−6)	1.071(−13)
HO ₂	5.71(−10)	5.66(−9)	1.406(−11)
H ₂ O	4.00(−2)	3.99(−2)	5.768(−5)
N ₂	7.74(−1)	7.74(−1)	7.995(−1)
NO	1.05(−4)	1.24(−4)	1.003(−11)
NO ₂	6.77(−5)	4.18(−5)	6.027(−12)
NO ₃	4.52(−8)	2.61(−8)	3.598(−15)
N ₂ O ₅	0	0	1.65(−13)
HNO	6.07(−15)	7.09(−14)	0
HNO ₂	1.07(−6)	1.66(−6)	3.879(−14)
HNO ₃	6.26(−10)	3.73(−10)	2.271(−10)
SO ₂	4.76(−9)	5.21(−6)	3.793(−9)
SO ₃	3.78(−10)	4.47(−7)	0
HSO ₃	1.25(−13)	1.51(−10)	0
H ₂ SO ₄	5.54(−11)	6.51(−8)	5.06(−13)

Note: $A(n)$ corresponds to $A \times 10^n$.

than 1.37. This means that, if in the combustion products there were no H₂SO₄ or SO₂ which could be converted into H₂SO₄ in the plume, no condensation of the H₂O vapor would occur. This was previously noted in [14], where the condensation processes in the plume of a B-707 aircraft were calculated along the stream tubes.

On the other hand, supersaturation in the H₂SO₄ vapor ($S_2 > 1$) is realized in most of the plume for $[S]_f = 0.04\%$ and, in the absence of sulfur in the fuel ($[S]_f = 0\%$), near the plume edge, with the maximum supersaturation being equal to 1.4 (Fig. 2). For $[S]_f = 0.04\%$, the maximum value of S_2 is attained at $x = 20$ m and is equal to 42. It should be noted that in the stream tube corresponding to the boundary of the first and second engine ducts, for $[S]_f = 0.04\%$ even at a distance of 4 m from the nozzle outlet large values of S_2 ($S_2 = 8$) are attained. On the plume axis, values of $S_2 > 1$ are realized at much greater distances from the nozzle outlet ($x \geq 35$) m. The presence of these high supersaturations in the H₂SO₄ vapor results in binary (H₂O/H₂SO₄) nucleation and the appearance of nuclei (their radius depends on the value of S_2 and amounts to 0.4–0.5 nm). Nucleation starts on the stream tube corresponding to the boundary of the first and second engine ducts and in the region of the outer thermal boundary of the plume, very near the nozzle outlet ($x = 4$ m) (Fig. 3). The thermal boundary of the plume is determined by the position of the point nearest to the axis at which the condition $|(T - T_\infty)/(T_0 - T_\infty)| \leq 0.01$ is satisfied, where T_0 and T_∞ are the temperature on the jet axis and in the ambient atmosphere. In this case, the sulfate aerosol concentration N_d in the section $x = 4$ m at $r = 1$ is $3.6 \times 10^6 \text{ cm}^{-3}$.

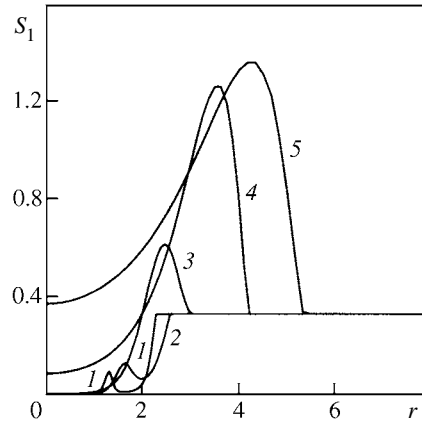


Fig. 1. Radial variation of the supersaturation in water vapor S_1 in the plume sections $x = 4, 10, 20, 40$, and 60 m (1)–(5).

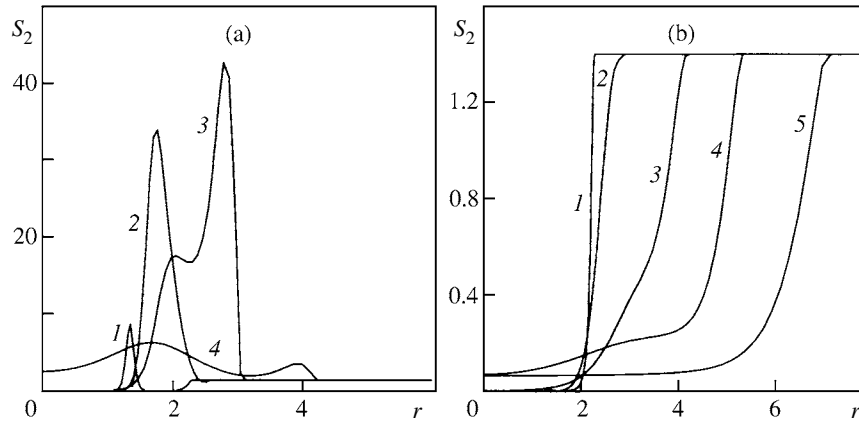


Fig. 2. Radial variation of the supersaturation in H_2SO_4 vapor S_2 in the plume sections $x = 4, 10, 20, 40$ m (1)–(4) for $[S]_f = 0.04\%$ (a) and $x = 4, 20, 40, 60, 100$ m (1)–(5) for $[S]_f = 0\%$ (b).

With increase in the distance from the nozzle outlet, the gas is cooled, the nucleation region expands, and the sulfate particle concentration increases. Thus, for example, at $x = 10$ m the maximum value $N_d = 2 \times 10^9 \text{ cm}^{-3}$ is attained at $r = 1.6$ m. At the same time, at $x = 20$ m the maximum value of N_d is attained at $r = 2$ and is equal to $\sim 7 \times 10^{10} \text{ cm}^{-3}$. It is interesting to note that on the jet axis ($r = 0$) nucleation starts only at $x \geq 35$ m but a noticeable number of aerosol particles ($N_d = 2 \times 10^7 \text{ cm}^{-3}$) appears on the axis even at $x = 15$ m and, at $x = 20$ m the particle concentration attains $1.6 \times 10^9 \text{ cm}^{-3}$. This is attributable to particle diffusion from the region lying on the boundary of the jets flowing out of the first and second engine ducts. This explains why in flight experiments small particles with a diameter $d \leq 2$ nm are registered at distances of 20–25 m from the nozzle outlet, although the quasi-one-dimensional models predict aerosol formation only at $x > 35$ –40 m.

The two-dimensionality of the aerosol particle formation is most clearly demonstrated in Fig. 4, which for $[S]_f = 0.04\%$ (a) and 0% (b) shows the boundaries of nucleation zone I (curves A, B, and C) and zones II and III, in which there is no nucleation. For any value of $x = \text{const}$ in the region $x < x_c$, the curves $N_d(r)$ have two maxima corresponding to the two segments of the nucleation zone separated by curve C. Curve B is the thermal boundary of the plume (since it is assumed that the turbulent Prandtl and Schmidt numbers are equal, H_2SO_4 and other components are not formed outside the plume). When there is no sulfur in the fuel, the boundaries of the nucleation region are displaced downstream. Thus, whereas for $[S]_f = 0.04\%$ nucleation starts on the axis at $x = 35$ m, for $[S]_f = 0\%$ it starts only at $x = 60$ m.

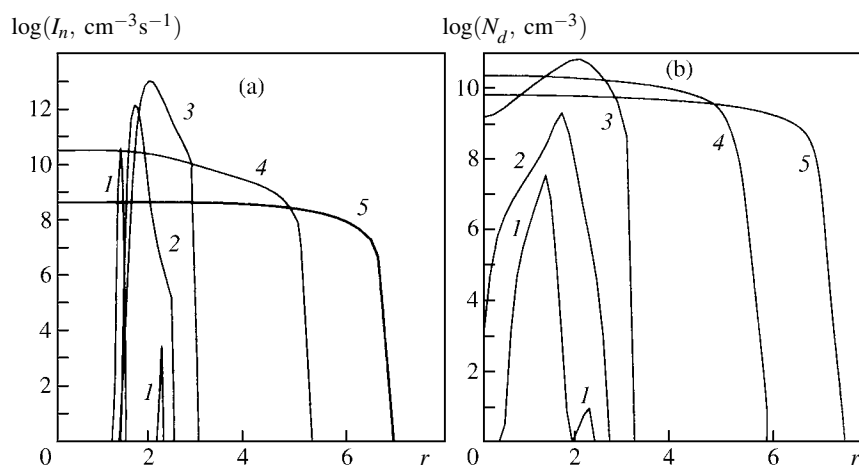


Fig. 3. Radial variation of the nucleation rate (a) and the aerosol concentration (b) in the plume sections $x = 4, 10, 20, 60, 100$ m (I)–(5) for $[S]_f = 0.04\%$.

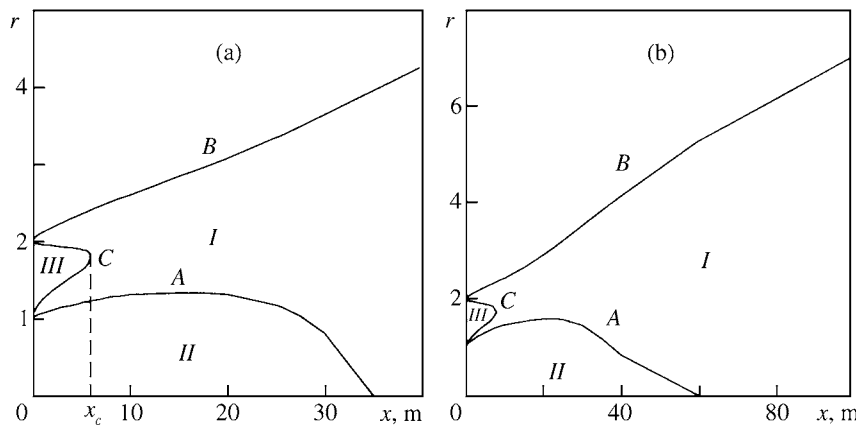


Fig. 4. Boundaries of the nucleation zone in the plume for $[S]_f = 0.04\%$ (a) and 0% (b).

The supersaturation and the nucleation rate are determined by the concentration of sulfuric acid vapor in the combustion products. The formation of H_2SO_4 is related mainly with the conversion of SO_2 into H_2SO_4 in the engine duct between the combustion chamber and the nozzle outlet [8, 16]. The conversion rate significantly depends on the gas parameters and the time spent by the gas inside the engine duct. This rate may vary from 2.5 to 10% [7]. However, SO_2 may also be converted into H_2SO_4 in the exhaust plume [9, 14–17]. This was confirmed by our calculations. On the plume axis, between the nozzle outlet and $x = 15$ m the concentration of H_2SO_4 increases by approximately 5 times due to the conversion $\text{SO}_2 \Rightarrow \text{SO}_3 \Rightarrow \text{H}_2\text{SO}_4$ (this is mainly the initial segment of the plume which is approximately 12.4 m long) (Fig. 5). The further decrease in concentration on the interval from 15 to 40 m is attributable to plume expansion. At $x \geq 40$ m, intense nucleation and drop growth resulting from heterogeneous condensation begin and by $x = 80$ m the H_2SO_4 concentration has decreased by a factor of 10^3 . The sulfuric acid propagates to the periphery due to diffusion from the boundaries of the first and second engine ducts. Here, its concentration is less than on the plume axis. However, since due to mixing with atmospheric air on the periphery of the plume the temperature decreases much faster than on the plume axis, nucleation starts on the periphery.

Since the maximum nucleation rate is realized in the mixing layer of the jets flowing out of the first and second engine ducts, in this region at small distances from the nozzle outlet (up to $x = 40$ m) the aerosol particle concentration is maximum. This is illustrated by Fig. 6. At $x > 60$ m, the aerosol concentration is almost constant over the entire region of the exhaust plume, i.e. the two-dimensional effects are manifested only at small distances from the nozzle outlet. We also note, that, when there is no sulfur in the fuel, the

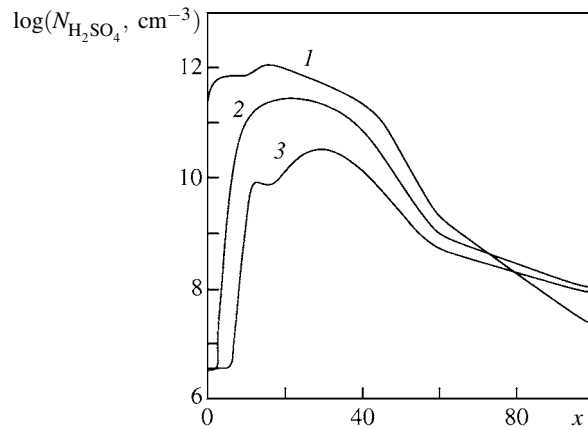


Fig. 5. Variation of the concentration of H_2SO_4 molecules in the mixture along the stream tubes corresponding to $r_0 = 0$, 1.5, 2 (1)–(3) for $[S]_f = 0.04\%$.

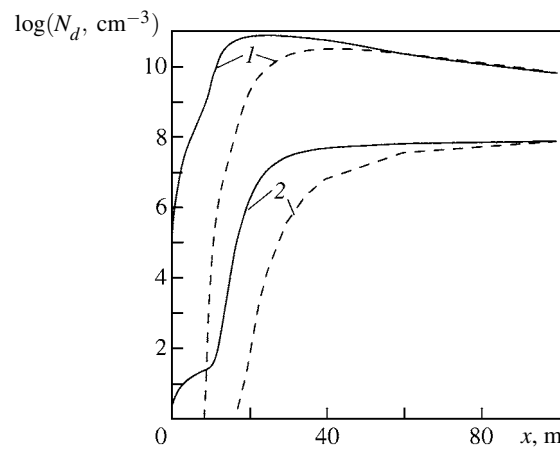


Fig. 6. Variation of the maximum and axial aerosol concentrations (N_d) along the plume axis (continuous and broken curves) for $[S]_f = 0.04\%$ and 0% (curves (1) and (2)).

concentration of sulfate aerosols in the plume is fairly high. For $[S]_f = 0\%$ the maximum value of N_d is $7.6 \times 10^7 \text{ cm}^{-3}$ (this is attained at $x = 100 \text{ m}$), which is $\sim 10^3$ times smaller than for $[S]_f = 0.04\%$ (for $[S]_f = 0.04\%$ the value $(N_d)_{\max} \approx 7.9 \times 10^{10} \text{ cm}^{-3}$ is attained at $x = 25 \text{ m}$). For $[S]_f = 0\%$ and $[S]_f = 0.04\%$, the size of the aerosol particles also differs significantly. The particle size is determined mainly by the coagulation of the nuclei formed and their condensation growth. For a sulfur percentage $[S]_f = 0.04\%$ and for $x > 20 \text{ m}$, the mean diameter of the aerosol particles increases with increase in the distance from the nozzle outlet and, at $x = 90 \text{ m}$, is $\sim 2 \text{ nm}$ (Fig. 7). The measurements demonstrated that at an average sulfur concentration $[S]_f = 0.027\%$ or more coarse particles with $d = 5 \text{ nm}$ and even 9 nm are present in the jet, but their concentration is much smaller than the concentration of the particles with $d = 2 \text{ nm}$ [6]. For a fuel that contains no sulfur the particle size is much smaller and is equal to 0.82 nm at $x = 90 \text{ m}$. Near the nozzle outlet ($x < 25 \text{ m}$), in the near-axis region there are only nuclei (there is almost no condensation of H_2O and H_2SO_4 vapor or coagulation in this region), which is why the size is mainly determined by the concentration of H_2SO_4 in the gas phase.

The analysis performed predicts the formation of ultrafine sulfate particles ($d \approx 1 \text{ nm}$) even in the case of fuels which contain no sulfur. This indicates that the environmental safety of using hydrogen as a fuel requires more thorough verification. The combustion of hydrogen is accompanied by substantial emission of oxides of nitrogen. The percentage of the H_2O vapor in the exhaust also turns out to be greater than when aviation kerosene is burned, which could result in the formation in the plume of aerosol particles consisting of an $\text{H}_2\text{O}/\text{H}_2\text{SO}_2/\text{HNO}_3$ solution.

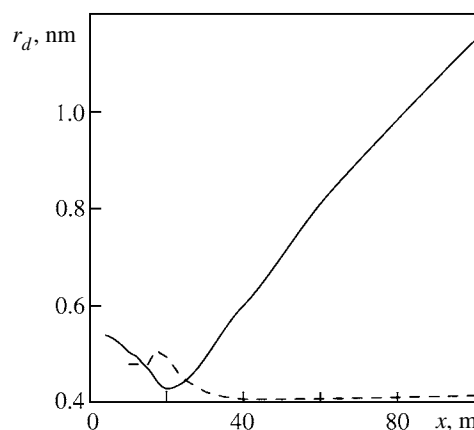


Fig. 7. Variation of the particle radius along the plume axis for $[S]_f = 0\%$ and 0.04% (broken and continuous curves).

Summary. A physico-mathematical model of the formation of liquid sulfate aerosols in the turbulent plume flowing from the nozzle of a two-duct engine of a modern wide-body aircraft is presented. The model includes the gasdynamical equations for a turbulent jet, the equations of chemical kinetics, the equations for the mass concentrations of H_2O and H_2SO_4 in the liquid phase, and the equation for the aerosol particle concentration and takes into account the volume nucleation, condensation growth, and coagulation of the particles formed. The model also takes into account such specific features of the flow considered as the nonuniform distribution of the gasdynamic parameters and component concentrations in the initial section of the plume leading to the development of a mixing layer (starting from the duct boundary), and the transverse diffusion of the mixture components and aerosol particles.

The topology of the zones of binary nucleation of water and sulfuric acid vapor in the exhaust plume of a wide-body jet aircraft is determined for the first time. Nucleation starts at very small distances from the nozzle outlet ($x \approx 4$) in the mixing layer of the jets from the first and second engine ducts. On the nozzle axis, nucleation starts at much greater distances from the nozzle outlet ($x \geq 35$ m), but due to the diffusion of small ($d = 1$ nm) aerosol particles from the mixing layer, large numbers of particles ($N_d \sim 10^9 \text{ cm}^{-3}$) appear on the nozzle axis even at a distance of 20 m from the nozzle outlet, which agrees well with the experimental data. The quasi-one-dimensional models used earlier for analyzing sulfate aerosol formation in jet engine plumes cannot explain this fact.

The work received financial support from the Russian Foundation for Basic Research (No. 05-01-00394) and the Presidential Council for supporting young scientists and leading science schools (grant NSH. 9320.20068).

The authors are grateful to A.M. Savel'ev for assisting with the calculations and for his helpful advice.

REFERENCES

1. C.P. Brasseur, R.A. Cox, D. Hauglustaine, I. Isacsen, J. Lelieveld, and D.A. Lister, "European Scientific Assessment of the Atmospheric Effects of Aircraft Emissions," *J. Atmos. Environ.* **32** (13), 2329–2418 (1998).
2. D.W. Fahey, U. Schumann, S. Ackermann, et al., "Aviation and the Global Atmosphere. A Special Report of the International Panel on Climate Change" (Ed. J.E. Penner et al.), Cambridge Univ. Press, New York (1999), 65–120.
3. O.B. Popovicheva, A.M. Starik, and O.N. Favorskii, "Problems of the Effect of Aviation on the Gas and Aerosol Composition of the Atmosphere," *Izv. Ross. Akad. Nauk, Fiz. Atmos. Okeana* **36** (2), 163–176 (2000).
4. U. Schumann, J. Ström, R. Busen, et al., "In Situ Observations of Particles in Jet Aircraft Exhausts and Contrails for Different Sulfur-Containing Fuels," *J. Geophys. Res.* **101**, No. D3, 6853–6869 (1996).
5. F.P. Achroder, B. Kärcher, R. Petzold, et al., "Ultrafine Aerosol Particles in Aircraft Plumes: In Situ Observations," *Geophys. Res. Lett.* **25** (15), 2789–2792 (1998).
6. C.A. Brock, F. Schröder, B. Kärcher, et al., "Ultrafine Particle Size Distributions Measured in Aircraft Exhaust Plumes," *J. Geophys. Res.* **105**, No. D21, 26.555–26.567 (2000).

7. U. Schumann, F. Arnold, R. Busen, et al. "Influence of Fuel Sulfur on the Composition of Aircraft Exhaust Plumes. The Experiments SULFUR 1-7," J. Geophys. Res. **107**, No. D15, 10.1029/2001JD000813 (2002).
8. R.C. Brown, R.C. Miake-Lye, M.R. Anderson, C.E. Kolb, "Effect of Aircraft Exhaust Sulfur Emission on Near-Field Plume Aerosols," J. Geophys. Res. Lett. **23** (24), 3607–3610 (1996).
9. B. Kärcher and D.W. Fahey, "The Role of Sulfur Emission in Volatile Particle Formation in Jet Aircraft Exhaust Plumes," *Geophys. Res. Lett.* **24**, No. 4, 389–392 (1997).
10. B. Kärcher, "Physicochemistry of Aircraft-Generated Liquid Aerosols, Soot, and Ice Particles: I. Model Description," J. Geophys. Res. **103**, No. D14, 17.111–17.128 (1998).
11. B. Kärcher, F. Yu, F.P. Schröder, and R.P. Turco, "Ultrafine Aerosol Particles in Aircraft Plumes: Analysis of Growth Mechanisms," *Geophys. Res. Lett.* **25** (15), 2793–2796 (1998).
12. F. Yu and R.P. Turco, "The Formation and Evolution of Aerosols in Stratospheric Aircraft Plumes: Numerical Simulations and Comparisons with Observations," J. Geophys. Res. **103**, No. D20, 25.915–25.934 (1998).
13. F. Yu, R.P. Turco, and B. Kärcher, "The Possible Role of Organics in the Formation and Evolution of Ultrafine Aircraft Particles," J. Geophys. Res. **104**, No. D4, 4079–4087 (1999).
14. R.C. Brown, R.C. Miake-Lye, M.R. Anderson, C.E. Kolb, and T.J. Resch, "Aerosol Dynamics of Near-Field Aircraft Plumes," J. Geophys. Res. **101**, No. D17, 22.939–22.953 (1996).
15. G. Gleitsmann and R. Zellner, "A Modeling Study of the Formation of Cloud Condensation Nuclei in the Jet Regime of Aircraft Plumes," J. Geophys. Res. **103**, No. D16, 19.543–19.556 (1998).
16. A.M. Savel'ev and A.M. Starik, "Dynamics of Sulfat Aerosol Formation in Engine Jets," *Fluid Dynamics* **36**, 95 (2001).
17. A.M. Starik, A.M. Savel'ev, N.S. Titova, et al., "Effect of Aerosol Precursors from Gas Turbine Engines on the Volatile Sulfate Aerosols and Ion Clusters Formation in Aircraft Plumes," *Phys. Chem. Chem. Phys.* **6** (5), 3426–3436 (2004).
18. A.B. Vatazhin, A.B. Lebedev, and V.A. Mareev, "Mathematical Modeling of Various Condensation Regimes in Turbulent Isobaric Jets," *Fluid Dynamics* **20** (1), (1985).
19. Z. Wang and J.-Y. Chen, "Modeling of Microscale Turbulence and Chemistry Interaction in Near-Field Aircraft Plumes," J. Geophys. Res. **102**, No. D11, 12871–12883 (1997).
20. L.I. Zaichik, A.B. Lebedev, A.M. Savel'ev, and A.M. Starik, "Modeling of Binary H_2O/H_2SO_4 Condensation in Jet Engine Plumes on the Basis of the Eulerian Fraction Method," *Teplofiz. Vys. Temp.* **38** (1), 81–90 (2000).
21. V.E. Kozlov, A.N. Sekundov, and I.P. Smirnova, "Models of Turbulence for the Description of a Flow in a Jet of a Compressible Gas," *Fluid Dynamics* **21**, 875 (1986).
22. A.B. Lebedev, A.M. Starik, and N.S. Titova, "Numerical Study of Nonequilibrium Photochemical Processes in a Subsonic-Aircraft Co-Current Plume," *Teplofiz. Vys. Temp.* **36** (1), 79–93 (1998).
23. A.B. Vatazhin, I.R. Safin, and E.K. Kholshchevnikov, "Investigation of Different Condensation Regimes in Iso-baric Turbulent Air-Steam Jets," *Fluid Dynamics* **37**, 877 (2002).
24. A.R. Avetisyan, V.M. Alipchenkov, and L.I. Zaichik, "Modeling of a Flow of Spontaneously Condensing Wet Steam in Laval Nozzles," *Teplofiz. Vys. Temp.* **40** (6), 937–946 (2002).
25. A.A. Samarskii, *Introduction to the Theory of Finite-Difference Schemes* (Nauka, Moscow, 1971) [in Russian].